RESEARCH ARTICLE

RSP Science Hub

International Research Journal on Advanced Science Hub
2582-4376
Vol. 03, Issue 08
www.rspsciencehub.com

Check for updates

http://dx.doi.org/10.47392/irjash.2021.233

Experimental Investigation on Machining of Nickel Chromium Alloy 718 using Abrasive Water Jet Machining

R Vijayakumar [1], *A Vasanth*[1], *M Nandhakumar*[1], *G Purushothaman*[1]

[1]*Assistant Professor, Department of Mechanical Engineering, GRT Institute of Engineering and Technology, Tiruvallur, 631209, Tamil Nadu, India*

Email: vijayrecruit8723@gmail.com

Article History

Received: 16 June 2021
Accepted: 18 August 2021

Keywords:

AWJM;
Inconel 718;
GRA and ANOVA

Abstract

Nickel-chromium alloy 718 has a wide range of uses in aerospace, defence, automotive, and civil engineering, among other fields. Using the Abrasive Water Jet Machining (AWJM) method to cut Inconel 718 and optimising parameters such as Abrasive mass flow rate (AMFR), Stand of Distance (SOD), and Traverse Speed, this study aims to reduce surface roughness and kerf angle (TS). Then 9 samples were chosen from a total of 27 for analysis. The machined material is subjected to CMM and surface roughness inspections in order to get the best surface roughness and kerf width values. With the aid of Grey Relation Analysis (GRA) and ANOVA, the characteristic change is tabulated and a graph is displayed. The Surface Roughness rating has been decreased from 3.489 μm to 4.687μm. Similarly, the kerf width value has been decreased from 1.983 mm to 2.559 mm. AWJM is an excellent choice for Because of its better physical and mechanical qualities, metal matrix is rapidly being employed in different applications such as space, aircraft, marine, architectural, and car sectors, despite their higher cost.

1. Introduction

In the nuclear, aerospace, and power generation industries, rapid global industrialization has resulted in a demand for novel materials that must be compatible. Inconel 718 is a high-yield strength, hardness, melting point, and heat resistance super alloy based on future advanced materials in the region above. Because of its resistance to oxidation and corrosion, the super alloy Inconel 718 is widely utilized in high-temperature applications.

Cutting composite/metallic crossover stacks with an AWJ presents a number of issues. Surface quality and surface morphology/respectability during rough water jet penetration of Ti6Al4V/CFRP stacks with diverse operating circumstances were explored in this study . The grating water jet Machining of both Inconel 625 and AISI 1040 steel is introduced, with an expect to comprehend the AWJ opening penetrating execution and to explore the cycle checking by utilizing acoustic emission (Prasad and Asthana). The fundamental preferred position of the AWJ is the nonattendance of the warmth influenced zone and its adaptability. Boring tests were performed on various materials and the opening profundity and distance across were seen at various machining times. It was discovered that when penetrating various materials with a consistent fly, the profundity and breadth of the opening increment with a force work (Rohatgi). By preserving three degrees of four-cycle boundaries—grating

stream rate, water pressure, gap distance, and cross speed—trials were designed using a response surface strategy box Behnken configuration. During machining, the surface inconsistency is calculated. The design professional program was used to create an updated numerical model of cycle boundaries in order to achieve the required surface unpleasantness test examination of machining conditions and apparatus math on a superficial level discomfort when turning Inconel 625 (R and Ramakrishnan). The utilization of MQL helped going prompts huge improvement in surface quality. There is almost 12 to 17% advancement of surface get done with use of MQL. The examination demonstrates that the instrument nose radius is the predominant factor influencing the surface harshness, alongside approach point and feed rate (Kipcak et al.). The three operating measures considered are abrasive water flow operation, crushing and treatment. The exposure of the TLBO calculation is concentrated with regard to convergence rate and exactness of the arrangement (Kara et al.).

Water stream jet pressure, gap distance, and abrasive mass stream rate are the cycle parameters. The variation of individual reactions is examined to identify the example in which each boundary impacts the cycle's presentation. Plots have been used to explain the connections between the various parts. The mean effects plot was obtained by examining the means. The findings of the difference and means investigations were considered, and a strong link was discovered (Bonnet et al.). The optimal selection of process parameters is critical for guaranteeing product quality, lowering processing costs, and boosting processing productivity. Advanced machining technology (also known as abrasive water jet processing technology) and two major traditional processing technologies, namely grinding and milling, are among the three processing technologies whose process parameters are optimized (Gupta and Satyanarayana). Four process parameters-distance, pressure, abrasive grain size and elapsed time were measured in the study. The key parameters were determined and their influence on MRR and cone angle was discussed. The results obtained show that MRR is most impacted by the size and distance of abrasive particles (Sudhakar). Six diverse process parameters were utilized and their communications were created to portray the math of the cavity shaped by the abrasive water stream. The shape of machining area is defined by the depth of cut, at which the quadratic term of hydraulic pressure is considered the main influence. With different parameters fixed, two distinctive pressure ranges can be utilized to create a similar profundity of cut. This is identified with power utilization and framework wear. The feed rate has no huge impact on the profundity of cut; hence, it tends to be improved to build profitability using (Shirvanimoghaddam). It has been shown that several researchers employed and optimized processing parameters such as travel speed, water jet pressure, contact distance, abrasive mesh size, and abrasive mass flow rate on a regular basis. It is essential to study beforehand the changes in diameter of the nozzle and the orifice, the angle of impact of the jet, the size of the abrasive and abrasive mixture (mixture of different abrasives). Current studies have shown that it is recommended to use oblique jet impact angles for processing materials with high penetration depth, small taper cutting angle and improved surface quality (Manjunatha, Niranjan, and Satyanarayana). The Inconel 625 was machined utilizing a rough water jet machining measure. The main input parameters (such as pressure, distance and abrasive flow rate) have been changed to accomplish the ideal output parameters, namely blank removal rate, roundness, taper angle and surface harshness (Gangolu et al. Han and Chen). Grey relational analysis has been effectively used to improve the process in several non-traditional machining processes, thus an attempt has been made to use grey relational analysis for the abrasive water jet drilling process.

2. Materials and Methods

Inconel is known for its high tensile strength, high impact resistance, and high resistance to rupture. Both cryogenic and non-cryogenic uses are possible with this super alloy. The Chemical composition of Inconel 718 is revealed in Table-1. Mechanical properties of Inconel 718 are shown in Table-2. Characteristics at high temperatures (700°C) and cryogenic temperatures (about 250°C). Material for Inconel 718 was acquired in 99.99 percent pure form from India Mart in Mumbai, India. A CNC machine Waterjet Germany S3015 with a working bed size of 3200* 1700 mm and an Inconel 718 nickel-based

alloy plate with dimensions of 150*150*10 mm. The X, Y, and Z axis travel are 3000 mm, 1500 mm, and 200 mm, respectively, with table height 910 mm. The highest operating pressure is 400 MPa, produced by a 37 KW engine. During the cutting operation, four process parameters such as water pressure, SOD, abrasive flow rate (AFR), and traverse speed were changed, while the jet. impact angle (90°), garnet abrasive size (80 mesh), and focusing tube diameter (1.1 mm) remained constant.

Abrasive water jet machining is used to cut Inconel 718 by changing parameters such as abrasive flow rate, transverse feed rate, and standoff distance. Figure 1. displays that the Inconel 718 (75*75*10 mm). Figure 2. shows the Inconel 718 after Machining and Figure 3. shows the material after cutting for roughness measurement by showing array of 27 samples. The set of 27 samples is prepared with different combination of parameters.

Then out of 27 samples, 9 samples were analyzed to find out the cut surface roughness and kerf characteristics.The characteristic change is Tabulated and graph is plotted

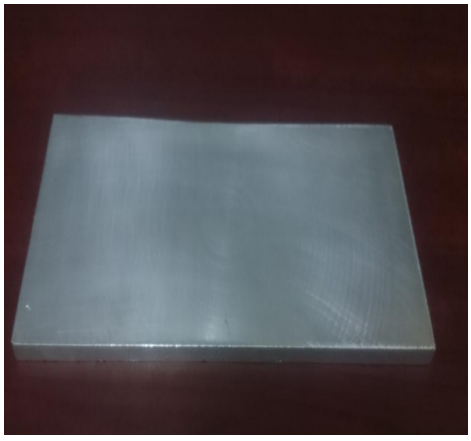


FIGURE 1. Inconel 718 Machining

In the illustration above, the machined work piece is plainly visible. Variables such as Jet traverse speed, Abrasive flow rate, and Stand-off distance are used in a series of 27 tests. Below are the cutting parameters with three levels of variation. The input process parameters for machining Inconel 718 and cutting parameters of experimental samples with their ranges are listed in Table-3. Finally, Table-4. Shows the test results and response values for multiple experiments.



FIGURE 2. Inconel 718 after Machining

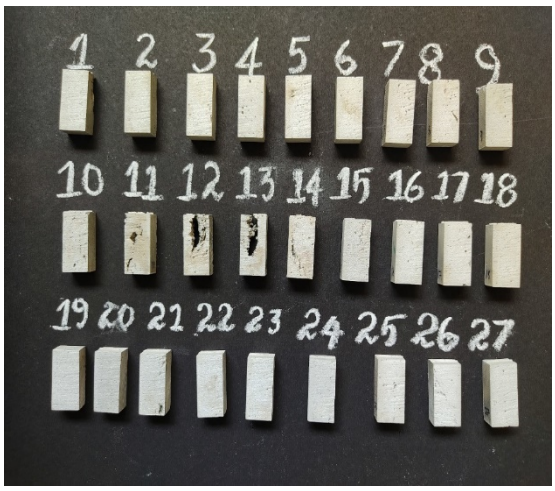


FIGURE 3. Array of 27 Samples

3. Test Results

The SURFCORDER and Video Measuring Systems are used to assess surface roughness and Kerf width, respectively. The outcomes are shown in the table below. Two experimental samples are cut using each of the Test settings, with the results labelled R1 and R2. The average figure is then used to do additional research. The water pressure is kept constant at 400 MPa throughout the experiment.

3.1. Surface Roughness Measurement

Surface roughness, often known as roughness, is a measurement of a surface's texture. The vertical deviations of an actual surface from its ideal form are used to evaluate it. The surface is rough if these variances are substantial; the surface is smooth if they are modest. Roughness may be determined by comparing it to a "surface roughness comparator," which is a sample of known surface roughness, but

TABLE 1. Chemical composition of Inconel 718

Element	Weight %	Comment
Ni	58 - 71 %	
Cr	21 – 23 %	
Mo	8 – 10 %	
Fe	5 %	Max
Nb	3.2 – 3.8 %	Nb+ Ta
Ti	0.3	
C	0.005	

TABLE 2. Mechanical properties of Inconel 718

Formand Condition	Tensile Strength (Mpa)	Yield Strength (Mpa)	Elongation(%)	Reduction of Area (%)	Hardness Brinell
Rod / Bar / Plate	827-1103	414-758	60-30	60-40	175-240
Sheet / Strip	827-1034	414-621	55-30	—	145-240
Tube and Pipe	827-965	414-517	55-30	—	—

TABLE 3. Cutting Parameters of Experimental Samples

Symbols	Parameters	Unit	Level 1	Level 2	Level 3
A	Traverse Speed	mm/min	60	80	100
B	Abrasive Mass Flow Rate	Kg/min	0.30	0.40	0.50
C	Stand of Distance	mm	1	2	3

TABLE 4. Test Result

Trail	Abrasive mass flow rate (Kg/min)	Traverse Speed (mm/min)	Stand of Distance (mm)	Surface Roughness (μm)			Kerf width (mm)		
				Trail 1	Trail 2	AVG	Top Kerf	Bottom kerf	AVG
1	0.35	64	1	3.75	3.872	3.811	1.895	1.282	1.755
2	0.35	64	2	3.91	4.026	3.968	1.905	1.196	2.030
3	0.35	64	3	4.05	4.165	4.107	1.975	1.251	2.073
4	0.35	80	2	4.07	4.192	4.131	1.868	1.12	2.141
5	0.35	80	3	4.05	4.171	4.110	2.015	1.158	2.453
6	0.35	80	1	4.45	4.570	4.51	1.795	1.25	1.560
7	0.35	96	3	4.41	4.530	4.47	1.905	1.028	2.510
8	0.35	96	1	4.62	4.736	4.678	1.965	1.071	2.559
9	0.35	96	2	4.52	4.640	4.58	1.87	1.08	2.262

more broadly a standard. Surface profiles are measured using a profilometer, which can be either contact (usually a diamond type) or optical (often a laser style) (e.g., a white light interferometer).

The Surface Roughness of the surface can be measured from SURFCORDER SE 3500 as shown in Figure 4.

3.2. Kerf Width

The breadth of material removed by a cutting operation is known as a kerf. The kerf width is determined by a variety of machining variables. Machines using video measuring systems is shown in Figure 5 are developed for non-contact examination and measurement of small complex details on small or big



FIGURE 4. Surfcorder SE3500

objects. From measuring microscopes and optical comparators, these video measurement devices are a natural progression.



FIGURE 5. Video Measuring System F 2010

4. Grey Relational Analysis and Anova

The signal to noise ratio (S/N Ratio) has been utilized as the quality parameter of choice in the field of communication engineering. Taguchi, who came from a background in communication and electrical engineering, used the same approach to experiment design. Taguchi has used the audio idea of signal-to-noise ratio (S/N Ratio) to a wide range of studies. Multi factor experiments are a common name for these types of investigations.

The S/N ratio is calculated using the smaller-is-better method, and the normalized S/N ratio is calculated using the larger-is-better formula, as shown in the table below.

STEP 1:

i. **Larger-the-Better**

The quality criterion is continuous and non-negative in this case, meaning it can take any value between 0 to ∞. Its goal value should be non-zero and as large as feasible.

S/N Ratio (η) = $-10\log_{10}\left(\frac{1}{r}\right)\sum_{i=1}^{r}\frac{1}{Y_{ij}^{2}}$ ... (1)

Where, r = number of replications

ii. Smaller-the-Better

The smaller-is-better characteristic is a non-negative, continuous measurable feature that can have any value between 0 to ∞.

S/N Ratio (η) = $-10\log_{10}\left(\frac{1}{r}.\sum_{i=1}^{r}Y_{ij}^{2}\right)$ ... (2)

iii. Nominal-the-Best

A user-defined goal value is assigned to a nominal-the-best feature. Equation is used to determine the S/N ratio (yij) for such an equation (3)

$$\frac{S}{N}\ ratio\ (\eta) = 10\ log_{10}\left(\frac{\mu^2}{\sigma^2}\right) \quad .....(3)$$

$$\mu = \frac{y_1+y_2+\cdots+y_r}{r}$$

$$\sigma = \sum_{i=1}^{r}\frac{\left(y_i-\bar{y}\right)^2}{r-1}$$

Where,

r = number of replications. m = number of observations.

y_{ij} = observed response values. i = 1,2,3... r; and j = 1,2,... m;

STEP 2:

Calculate the Normalized S/N ratio (Z_{ij}) using Equation (4) to eliminate the variability among the S/N ratio values of responses.

$$Z_{ij} = \frac{y_{ij} - \min(y_{ij}, i = 1,2,.....,n)}{\max(y_{ij}, i = 1,2,.....,n) - \min(y_{ij}, i = 1,2,.....,n)}$$

..... (4)

Where n is the number of trials.

STEP 3:

Compute the Grey Relational Coefficient (γ) from the normalized S/N ratio values using equation (5):

$$\gamma_i^j = \frac{\Delta\min + \xi\Delta\max}{\Delta_{oj}(i) + \xi\Delta\max}$$

.... (5)

Where,

i=1, 2....n; j=1,2....m;
n is the number of responses
m is the number of trials

$\Delta_{oj} = \|z_o(i) - z_j(i)\|$ is the absolute value of the difference between $z_o(i)$ and $z_j(i)$.

$z_o(i)$ is the reference sequence ($z_o(i)$=1; i=1,2,...,n)

$z_j(i)$ is the specific comparison sequence.

$\Delta \min = \min_{\forall j \neq i} \min_{\forall i} \|z_o(i) - z_j(i)\|$ is the smallest value of $z_j(i)$

$\Delta \max = \max_{\forall j \neq i} \max_{\forall i} \|z_o(i) - z_j(i)\|$ is the largest value of $z_j(i)$

ξ is the distinguishing coefficient whose value is taken to be 0.25 to ensure the equal importance for all the responses.

STEP 4:

Calculate the weighted GRG value using the equation (6)

$$GRG_i = \frac{1}{n}\sum_{i=1}^{n}(\gamma_i) \ldots\ldots (6)$$

The signal-to-noise ratio and normalized S/N ratio is displayed in Table 5. The Grey relation coefficient and Grey relation grade is tabulated in Table 6. Finally, the optimum level of individual parameters is displayed in Table 7. The grey relation grade is calculated and tabulated and a graph is plot for the values obtained. In Figures 6, 7, & 8 are showing the effects on pressure, standoff distance and traverse feed on output responses.

TABLE 5. S/N Ratio and Normalized S/N Ratio

SN ratios		Normalized SN ratio	
SR	BA	SR	BA
-11.6234	-4.2916	1.0000	0.7423
-11.9680	-5.2484	0.8058	0.4377
-12.2679	-5.3849	0.6369	0.3942
-12.3241	-5.5880	0.6052	0.3296
-12.2806	-6.3769	0.6297	0.0785
-13.0843	-3.4819	0.1769	1.0000
-13.0069	-6.5420	0.2205	0.0259
-13.3982	-6.6234	0.0000	0.0000
-13.2187	-5.9280	0.1011	0.2213

TABLE 6. Grey Relation Co-efficient and Grey Relation Grade

Grey Relational Co-Efficient (GRC)		Grade (GRG)
SR (GRC)	Kerf (GRC)	
1.0000	0.6599	0.8299
0.7203	0.4707	0.5955
0.5793	0.4522	0.5157
0.5588	0.4272	0.4930
0.5745	0.3517	0.4631
0.3779	1.0000	0.6889
0.3908	0.3392	0.3650
0.3333	0.3333	0.3333
0.3574	0.3910	0.3742

TABLE 7. Optimum level for individual parameters

Factors	Level 1	Level 2	Level 3	max-min
A	0.6470	0.5484	0.3575	0.2895
B	0.5626	0.4640	0.5263	0.0987
C	0.6174	0.4876	0.4479	0.1695

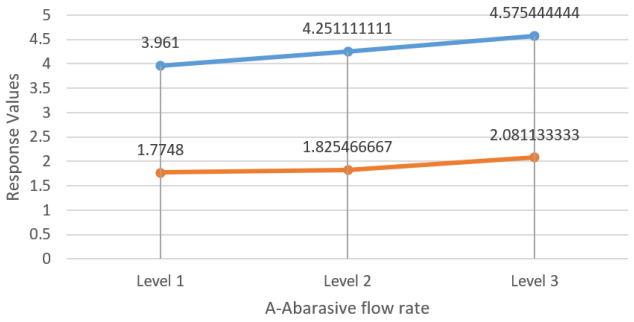


FIGURE 6. Effect of Abrasive flow rate on Kerf width and Surface Roughness.

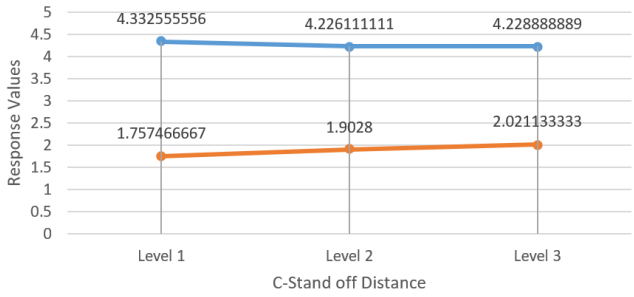


FIGURE 7. Effect of Stand of distance on Kerf width and Surface Roughness

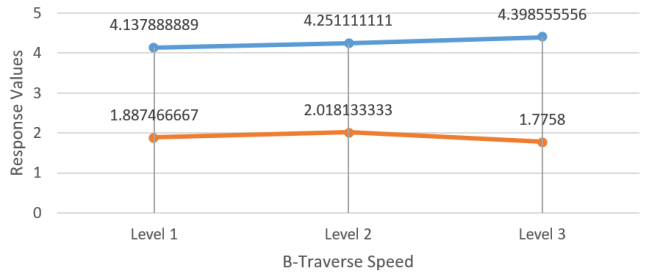


FIGURE 8. Effect of Traverse speed on Kerf width and Surface Roughness

5. SEM Image

Scanning using electrons microscopic images of the cut surface of the samples are taken to analyze the dispersion of the Boron carbide particle on the work sample. The SEM image of Inconel 718 for various input parameter combinations is shown in Figure 9. In comparison to trail 2 and trail 3, the surface roughness of the Inconel 718 sample from trail 1 has the highest value. The ploughing of Inconel 718 takes occur due to the greater value of jet transverse speed, 96 mm/min. The surface roughness of Inconel 718 and jet transverse speed of 96 mm/min are shown in Figure 7 and reduces as the transverse speed of the jet.

6. ANOVA

The basic goal of analysis of variance (ANOVA) is to determine the influence of specific components using a statistical approach. The influence of each component on the experimental findings may be determined very clearly using ANOVA data. Because the Taguchi experimental technique was unable to assess the impact of specific factors on the overall process, to account for this impact, an ANOVA was used and shown in Table 8. The total sum of squared deviations, or SST, is split into two parts. the sum of the squared errors and the total of each process parameter's squared variances the percentage contribution of each process parameter to the total sum of squared deviations SST may be used to assess the impact of changing a process parameter on performance attributes. When the F value is substantial, a change in the process parameter usually has a considerable impact on the performance characteristic. The parameter symbols typically used in ANOVA are described below: Source. The source includes the controlling factors A, B, C, and the error factor, e, and the sum of all observation, TSS

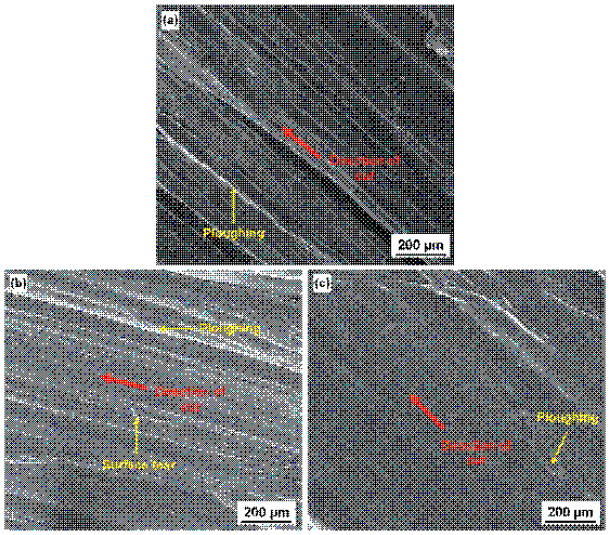


FIGURE 9. SEM image of Inconel 718 at different combination of input parameters ANOVA

(Sum of Squares). SSA, SSB, SSC... denote the sum of the squares of A, B, C... SSe denotes the error sum of squares; SST denotes the total variation. Thus, the equation can be written as:

SST (Total Variation) $=\sum_i^n = 1\ GV^2 - \ CF\ \ldots$ (7)

SS factor (Factor Variation) $=\sum_i^n = 1\ K_j(AGV)^2$ –CF .... (8)

Where, CF (Correction Factor) $=(\sum_i^n 1\ GV\}\ \frac{2}{N}\ldots$ (9)

GV = Grey relational Grade Value

n = Total number of experiments

m = Number of levels

AGV = Average Grade Value

K = Number of observations considered for calculating AGV

The ANOVA table with individual parameter contribution is shown below:

The anticipated optimal condition is determined using the additive model below. Figure 10 shows the contribution of various parameters. Predicted and experimental values are displayed in table 8. The final stage is to forecast and the quality characteris-

TABLE 8. ANOVA Table

Factor	SS	Dof	MS	F	% Contribution
A	0.1300	2	0.0650	32.0786	60.6394
B	0.0149	2	0.0075	3.6866	6.9689
C	0.0471	2	0.0236	11.6354	21.9949
Error	0.0223	11	0.0020		10.3968
Total	0.21434717				100

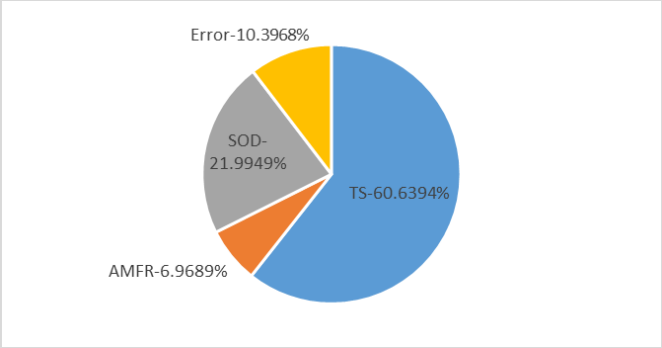


FIGURE 10. Contribution of various parameters

tic utilizing the ideal level of the design parameters once the optimal level of the design parameters has been determined. The factor levels obtained from Equations 8 and 9 are applied in this case. The estimated S/N ratio may be determined using the optimal level of design parameters as follows:

$\hat{\eta}=\eta_m + \sum_{i=1}^{q}\left(\bar{\eta}_i \eta_m\right)$

η_m= Average S/N ratio

η=Average S/N ratio corresponding to i^{th} factor on j^{th} level

q= number of factors

The predicted S/N ratio and the corresponding response is calculated and tabulated below:

TABLE 9. Optimum S/N ratio and Response

Parameters settings	GRG	Response	
		SR (μm)	Kerf width(mm)
Initial settings (A_3 B_2 C_1)	0.3333	4.678	2.559
Optimal Setting using GRA (A_1 B_1 C_1)	0.3855	3.489	1.983
Percentage	15.67%	125.41%	22.50%

Conclusion

The Inconel 718 material was machined 27 slots using Abrasive Water Jet Machining (AWJM) by varying parameters. Using Grey Relation Analysis and ANOVA, the optimal level is chosen as A1 B1 C1. (Abrasive flow rate of 0.35 Kg/min, Jet traverse speed 65 mm/min and Stand-off distance of 1 mm). At optimal level the GRG value is improved by 15.67 %. The Surface Roughness value is reduced to 4.687 μm from 3.489 μm. similarly, kerf width value is reduced to 2.559 mm from 1.983mm. Surface Roughness is minimized at lower traverse speed. The higher abrasive flow rate and lower stand-off distance yields better surface finish.

ORCID iDs

R Vijayakumar https://orcid.org/0000-0002-7005-0180

References

Gangolu, S, et al. "Effects of temperature and strain rate on compressive flow behavior of aluminum-boron carbide composites". *Journal of Composite Materials* 48.11 (2014): 1313–1321. 10.1177/0021998313485265.

Gupta, Nikhil and K. G. Satyanarayana. "The solidification processing of metal-matrix composites: The Rohatgi Symposium". *JOM* 58.11 (2006): 92–94. 10.1007/s11837-006-0236-0.

Han, Yu-Mei and X. -Grant Chen. "Electrochemical Behavior of Al-B4C Metal Matrix Composites in NaCl Solution". *Materials* 8.9 (2015): 6455–6470. 10.3390/ma8095314.

Kara, Ü., et al. "Performance of Boron-Carbide as Radiation Shielding". *Acta Physica Polonica A* 128.2B (2015): 10.12693/aphyspola.128.b-335.

Kipcak, A. Seyhun, et al. "Characterization of boron carbide particles and its shielding behavior against neutron radiation". *Energy Conversion and Management* 72 (2013): 39–44. 10.1016/j.enconman.2012.08.026.

Manjunatha, B., H. B. Niranjan, and K. G. Satyanarayana. "Effect of mechanical and thermal loading on boron carbide particles reinforced Al-6061 alloy". *Materials Science and Engineering: A* 632 (2015): 147–155. 10.1016/j.msea.2015.02.007.

Prasad, S. V. and R. Asthana. "Aluminum Metal–Matrix Composites for Automotive

Applications: Tribological Considerations". *Tribology Letters* 17.3 (2004): 445–453. 10.1023/b:tril.0000044492.91991.f3.

R, K and R Ramakrishnan. "Tribological Behaviour of Aluminium Hybrid Metal Matrix Composite". *Procedia Engineering* 97 (2014): 660–667. 10.1016/j.proeng.2014.12.295.

Rohatgi, P K. "A Surface-Analytical Study of Tribodeformed Aluminum Alloy 319-10 Vol.% Graphite Particle Composite". *Materials Science and Engineering: A* 123.2 (1990): 213–218. 10.1016/0921-5093(90)90286-c.

Shirvanimoghaddam, K. "Boron Carbide Reinforced Aluminium Matrix Composite: Physical, Mechanical Characterization and Mathematical Modelling". *Materials Science and Engineering: A* 658 (2016): 135–149. 10.1016/j.msea.2016.01.114.

Sudhakar, I. "Ballistic Behavior of Boron Carbide Reinforced AA7075 Aluminium Alloy Using Friction Stir Processing - an Experimental Study and Analytical Approach". *Defence Technology* 12.1 (2016): 25–31. 10.1016/j.dt.2015.04.005.



© Vijayakumar et al. 2021 Open Access. This article is distributed under the terms of the Creative Commons Attribution 4.0 International License (http://creativecommons.org/licenses/by/4.0/), which permits unrestricted use, distribution, and reproduction in any medium, provided you give appropriate credit to the original author(s) and the source, provide a link to the Creative Commons license, and indicate if changes were made.

Embargo period: The article has no embargo period.

To cite this Article: , R Vijayakumar, A Vasanth, M Nandhakumar, and G Purushothaman. "**Experimental Investigation on Machining of Nickel Chromium Alloy 718 using Abrasive Water Jet Machining**." International Research Journal on Advanced Science Hub 03.08 (2021): 176–184. http://dx.doi.org/10.47392/irjash.2021.233